Biogeochemistry **55:** 1–27, 2001.

Bacteria, diatoms and detritus in an intertidal sandflat subject to advective transport across the water-sediment interface

ANTJE RUSCH[1*], STEFAN FORSTER[1,2] & MARKUS HUETTEL[1]
[1]*Max Planck Institute for Marine Microbiology, Celsiusstr. 1, D-28359 Bremen, Germany;*
[2]*present address: Institute of Baltic Sea Research (IOW), P.O. Box 301161, D-18112 Rostock, Germany (*Author for correspondence, e-mail: arusch@mpi-bremen.de)*

Key words: bacteria, diatoms, intertidal sandflat, North Sea, particle transport, sediment-water interface

Abstract. This study focused on organic particles with respect to their transport and sedimentary mineralisation in a North Sea intertidal sandflat previously characterised as strongly influenced by advective transport across and below the water-sediment interface. Measured permeabilities of the sandy sediment ranged from 5.5 to $41 \cdot 10^{-12}$ m^2, and permeabilities calculated from granulometric data exceeded the measured values by a factor of 4.4 ± 2.8. Bacteria (2–9% of the POC) were highly variable in space and time. They were less mobile than interstitial fine (< 70 μm) organic and inorganic particles, as part of the population lived attached to large, heavy sand grains. The vertical distribution of bacteria was closely related to the organic carbon content of the fine-grained interstitial material. In winter, bacterial numbers in the uppermost 5 cm amounted to 39–69% of the summer ones. Carbon mineralisation rates ranged between 20 mg C m^{-2} d^{-1} in winter and 580 mg C m^{-2} d^{-1} in summer, keeping step with finer-grained sediments that contained an order of magnitude more organic carbon. Sedimentary carbohydrates were mainly intracellular or tightly bound to particles, and their concentrations were depth-invariant in winter, but exponentially decreasing with depth in summer. Below 5 cm depth, the mean concentration was (1590 ± 830) μg cm^{-3}, without major downcore or seasonal changes. Phytobenthos and phytodetritus were dominated by diatoms and comprised merely minor amounts of other primary producers. Planktonic diatom depth profiles were related to weather and phytoplankton conditions, and benthic diatoms showed similar depth distributions due to passive and active motion. The penetration of relatively fresh phytodetritus down to at least 5 cm, shown by chloropigment composition, emphasised the close coupling between water column and sandy sediment, facilitated by advective interfacial and subsurface flows.

Introduction

Intertidal zones are part of the highly dynamic nearshore shelf seas, where fluid motions associated with currents and surface waves reach down to

the sea floor and interact with the bottom sediments. In unprotected areas, small and light particles are frequently removed from the sediment, and thus permeable sands are the prevalent sediment type (Flemming & Ziegler 1995; Gätje & Reise 1998). They allow for advective transport of solutes (Huettel & Gust 1992; Forster et al. 1996; Ziebis et al. 1996) and particles (Huettel et al. 1996; Pilditch et al. 1998) across the water-sediment interface, when waves and bottom flows cause pressure gradients that force water through the upper sediment layers. The intensity of advective interfacial flow depends on the pressure gradient (Forster et al. 1996; Huettel et al. 1996) and permeability (Darcy 1856). The permeability of sands ranges between 10^{-12} m^2 and 10^{-10} m^2 and depends on grain size, sorting and compaction (Hsü 1989) as well as on viscosity and density of the pore fluid (Klute & Dirksen 1986). The present study was conducted in an intertidal sandflat with permeabilities in the upper 15 cm permitting advective exchange across the sediment surface under natural hydrodynamical conditions. In shallow water environments, bioirrigation and bioturbation can bring about high rates of solute and particle transport across the water-sediment interface. At our study site, however, less than half of the interfacial particle flux could be attributed to biogeneous transport, due to relatively low macrobenthic biomass (Rusch et al. 2000).

We conducted a one-year field study with the objective to demonstrate and understand the mechanisms that cause the spatial and temporal dynamics of particulate organic matter (POM) in the upper 10 cm of the sediment. We set out to prove our working hypothesis that in this sandflat permeability is a key factor for sedimentary POM dynamics by controlling advective transport of suspended matter between water column and sediment. Depth profiles of various pore water solutes strongly indicated advective interfacial transport (Rusch et al. 2000). We focused on benthic microbes, that not only mineralise organic matter, but also are mobile POM themselves, as are planktonic and benthic diatoms. Photosynthetic pigment analyses provided additional information on POM provenance and state of degradation. Quantities and distribution of extracellular mucopolysaccharides were measured, because they facilitate cell attachment and locomotion and reduce sediment permeability and erosion (Grant & Gust 1987; Decho & Lopez 1993; Yallop et al. 1994; Underwood et al. 1995). Finally we discuss interactions and correlations between the observed particle and sediment characteristics as well as biogeochemical and ecological implications of advective POM transport across the water-sediment interface.

Methods

Study site and sampling

Our study site was located in Königshafen Bay (55°02' N, 8°26' E) near Sylt island in the southern North Sea. At the sampling dates (17 Jul 97, 17 Sep 97, 18 Nov 97, 13 Jan 98, 15/17/19/23/25/27 Mar 98, 12 May 98 and 7 Jul 98), the intertidal sandflat was exposed to waves of less than 0.2 m amplitude and to currents of 0–0.32 m s^{-1}, measured 2 cm above the crest of up to 2 cm high ripples forming on the sediment surface. Benthic polychaetes were present in relatively low abundance; for details see Rusch et al. (2000).

At each sampling date, 1–1.5 h before low tide, we took 8 sediment cores of 6.0 cm i.d. and 1 core of 3.6 cm i.d., 20-40 cm long, from ripple troughs. Throughout the study, the respective sampling spots (0.5 m diameter) were chosen within the same selected circular area of 4 m radius. All time-sensitive procedures were performed in the nearby (500 m) lab immediately after sampling.

Sediment permeability and porosity

Of each core set, one core of 6.0 cm i.d. was cut at ca. 15 cm depth, and the lower, muddy part of the sediment column was discarded. The permeability k of the upper, sandy part was then determined by the constant head method (Klute & Dirksen 1986).

We compared these measurements with the permeabilities calculated according to three different empirical relationships suggested by Krumbein/Monk (Eq. 1, Hsü 1989), Carman/Kozeny (Eq. 2, Nield & Bejau 1992) and Hazen (Eq. 3, Eggleston & Rojstaczer 1998). To assess water content, grain size distribution and porosity, the core of 3.6 cm i.d. was sectioned in depth intervals of 0.25 cm (down to 1 cm), 0.5 cm (down to 2 or 4 cm) and 1.0 cm (down to 15 cm), and the slices were oven-dried at 70 °C for 48 h. We determined the water content W (in% w/w) from the weight loss upon drying and the grain size distribution by dry sieving. The porosity p_0 was calculated from the density of the sand, determined by Archimedes' method, the density of sea water, and W. The permeabilities k_{KM}, k_{CK} and k_H of the uppermost 10 cm were then calculated according to Equations 1, 2 and 3, respectively.

$$k_{KM} = 7.50 \cdot 10^{-4} \cdot d_{50}^2 \cdot e^{-1.31 \cdot \sigma(\phi)} \quad (1)$$

$$k_{CK} = p_0^3 \cdot d_{50}^2 / (180 \cdot (1 - p_0)^2) \quad (2)$$

$$k_H = 1.019 \cdot 10^3 \ m^{-2}s \cdot d_{10}^2 \cdot \nu \quad (3)$$

(with d_{50}: grain size median, d_{10}: first decile of the grain size distribution, $\sigma(\phi)$: standard deviation of grain sizes given in logarithmic ϕ units, ν: kinematic viscosity)

Bacteria, diatoms and carbohydrates

Of each core set, one core of 6.0 cm i.d. was sectioned in depth intervals of 0.5 cm (down to 2 or 4 cm) and 1.0 cm (down to 15 cm). From these slices we took aliquots of 1.0 cm^3, 1.5 cm^3, 0.2 cm^3 and twice 0.4 cm^3 for analysing bacteria, diatoms, total carbohydrates, water-soluble and EDTA-soluble carbohydrates, respectively.

Bacteria. 1 cm^3 of fresh sediment was added to 8 ml of NaCl solution (32 g l^{-1}) containing formalin (final concentration: 4%) and stored in the dark at 4 °C until analysis. Bacterial cells were dislodged from the sand grains by ultrasonic treatment, stained with DAPI, concentrated on polycarbonate membrane filters (0.2 μm pore size) and counted under epifluorescent illumination (Zeiss Axioskop), in all steps following the protocol suggested by Epstein and Rossel (1995). Using a magnification of 1300×, cell numbers were determined from two parallel filters per sample, in 5 randomly chosen counting grids each.

Diatoms. 1.5 cm^3 of fresh sediment was added to 6 ml of isohaline NaCl solution containing glutaraldehyde (final concentration: 1.6%) and stored in the dark at 4 °C until analysis. For the latter, the samples were suspended and the coarse particles (>70 μm) allowed to settle for 20 s, before the supernatant was decanted. After adding 4 ml of NaCl solution to the settled particles, they were once more treated alike. In a pre-test, the efficiency of extracting fine SiC particles from an artificial sand was 80–90% using this method. We examined the combined supernatant suspensions by light microscopy using a Fuchs/Rosenthal chamber and a magnification of 400×. Diatom frustules were counted separately as planktonic and benthic forms (Pankow 1990) and grouped into 5 length classes each: 10–15 μm, 15–20 μm, 20–25 μm, 25–30 μm and >30 μm.

Carbohydrates. Concentrations of total, water-soluble, and EDTA-soluble carbohydrates were assayed by the phenol/sulphuric acid method (Underwood et al. 1995).

Pigments

Of each core set, three cores of 6.0 cm i.d. were sectioned in depth intervals of 0.25 cm (down to 1 cm), 0.5 cm (down to 2 or 4 cm) and 1.0 cm (down to 15 cm). Parallel slices were pooled, gently suspended in isohaline NaCl solution, and allowed to settle. After 20 s, the supernatant was decanted and the remaining sediment once more retreated alike. The decanted suspensions, containing the particulate matter of an effective diameter less than 70 μm (hereafter referred to as "fine fraction"), were centrifuged (15 °C, 5 min, 1200·g). The pellet was freeze-dried, weighed and stored at 4 °C in the dark.

For pigment analysis, we prepared extracts from the fine fraction by dark incubation with 90% acetone at 4 °C for 16 h and subsequent centrifugation (4 °C, 7 min, 1620·g). The supernatant was syringe-filtered through 0.45 μm pores (Nalgene 199–2045 PTFE) and concentrated using a Savant SC 110A vacuum centrifuge.

20 μl of concentrated extract were separated on a Hypersil ODS C18 column using an HPLC system (Waters 600E gradient module, Waters 991 photodiode array detector/integrator). Solvents, gradients, flow rates and a detailed description of the method are given by Karsten and Garcia-Pichel (1996). Pigments were identified by their absorption spectra (350–800 nm) and retention times. The quantification of chloropigments and carotenoids was based on the peak areas at 410 and 440 nm, respectively. As calibration standards we used solutions of Chl a (Sigma), porphin (Sigma), canthaxanthin (Fluka) and the following carotenoids (^{14}C Agency Denmark): α-carotene, fucoxanthin, 19'-hexanoyloxyfucoxanthin, 19-butylfucoxanthin, lutein, and peridinin. Qualitative standard solutions of unknown concentrations were prepared of β-carotene, BChl a (*Rhodospirillium rubrum*), BChl c (*Prosthecochloris* spec.), chlorobactene (*Chlorobium vibrioforme*), and isoreniaratene (*Chlorobium phaeovibroides*). Other pigments were named operationally in the order of their retention times: chloropigments XA – XF and carotenoids YA – YF. The detection limit was an absorbance of 0.005 AU (absorbance units), corresponding to 110–330 ng pigment per cm^3 of sediment.

Rusch et al. (2000) determined total chloropigment concentrations fluorimetrically without acidification using a Hitachi F-2000. Solutions of Chl a in 90% acetone were used for calibration.

Porewater DIC and mineralisation rates

Porewater was obtained from the pooled parallel slices of 3 cores by centrifugation (500·g, 10 min, 15 °C) through GF-F filters in a Beckmann TJ-6 centrifuge, and 1.5 ml aliquots were kept at 4 °C in gas-tight glass vials containing 75 μl of $NaMoO_4$ (0.5 M). Dissolved inorganic carbon (DIC) was

Table 1. Permeability of the upper 10 cm of the sediment. k: measured values, k_{KM}: calculated according to Krumbein/Monk (Eq. 1), k_{CK}: calculated according to Carman/Kozeny (Eq. 2), k_H: calculated according to Hazen (Eq. 3). In Nov 97 and Jan 98, measurements were done in two parallel cores

	k (0-10 cm) in 10^{-12} m^2	k_{KM}/k	k_{CK}/k	k_H/k
17 Jul 97	15.0	2.94		2.09
17 Sep 97	40.7	2.35	1.92	2.09
18 Nov 97	18.7	2.37	4.90	2.73
18 Nov 97	6.7	6.60	13.7	7.61
13 Jan 98	10.8	3.60	4.94	3.93
13 Jan 98	12.4	3.20	4.26	3.24
17 Mar 98	23.0	1.66	1.56	1.98
19 Mar 98	9.4	4.08	4.90	4.11
23 Mar 98	13.6	2.81	1.84	3.64
25 Mar 98	5.5	9.53	6.44	11.9
27 Mar 98	6.7	5.53	6.84	5.30
12 May 98	10.3	3.77	7.54	3.77
7 Jul 98	34.2	1.82	2.78	1.78
mean		3.87 ± 2.21	5.13 ± 3.35	4.17 ± 2.82
median		3.20	4.90	3.64

measured using a flow-injection system, and mineralisation rates were estimated from the DIC depth profiles. For details see Rusch et al. (2000). Briefly, carbon mineralisation rates were calculated from DIC profiles according to three different approaches, B, C and D, by depth integration of DIC concentrations using three different background concentrations. Computations were based on the assumption that DIC accumulated between the time of highest near-bottom tidal current velocity and sampling.

Results

Sediment permeability

The measured permeabilities k and the calculated permeabilities k_{KM}, k_{CK} and k_H are listed in Table 1. There was a significant positive correlation between k and k_{KM} ($\alpha < 1\%$) and between k and k_H ($\alpha < 5\%$), with a slope of the regression line of 1.19 and 0.88, respectively. The slope of the regression

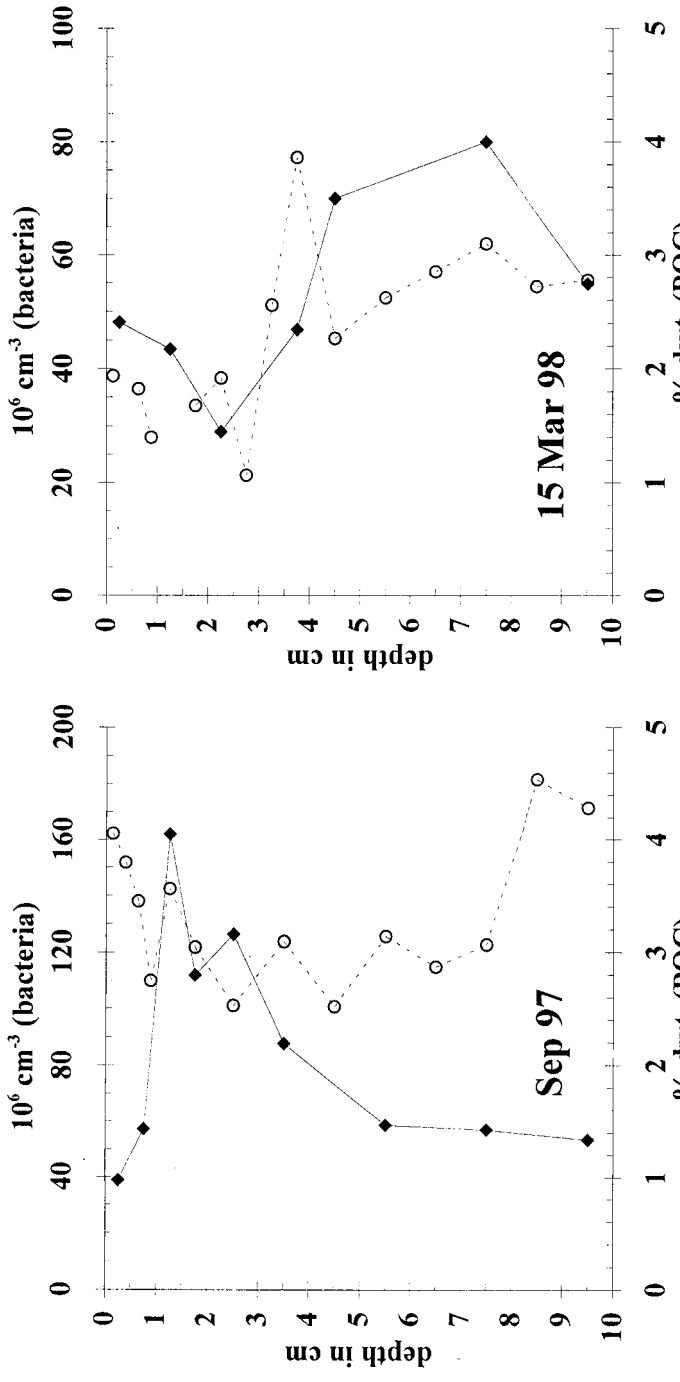

Figure 1. Depth profiles of bacterial cell numbers (diamonds) and POC content of the fine fraction (circles). Left panel: Sep 97 representing the summer situation; right panel: 15 Mar 98 representing the winter situation. The complete data set of all profiles is available from the authors.

Table 2. Maximum and minimum numbers of sedimentary bacteria, vertical gradient between minimum and subsurface maximum, and relative bandwidth, (max – min)/max, of cell numbers

	Maximum number 10^6 cm^{-3}	Minimum number 10^6 cm^{-3}	Gradient 10^6 cm^{-4}	(max – min)/max
Jul 97	215			
Sep 97	162	38.9	123	0.760
Nov 97	147			
Jan 98	95.0	34.3	60.8	0.640
Mar 98	97.5	36.0	36.9	0.405
May 98	99.7	53.0	54.3	0.545
Jul 98	112	74.7	96.6	0.785

line between k and k_{CK} was 0.88, the correlation lacking statistical significance, though. There was no seasonal trend in the measured or calculated permeabilities.

Porosities and grain size distributions depended on sediment depth ($\alpha < 5\%$, Wilcoxon matched pairs signed rank test, Sachs 1997):

$$d_{50}(0-2\text{ cm}) \approx d_{50}(10-15\text{ cm}) > d_{50}(2-5\text{ cm}) \approx d_{50}(5-10\text{ cm})$$
$$\text{and } p_0(0-2\text{ cm}) > p_0(2-5\text{ cm}) \approx p_0(5-10\text{ cm}) \approx p_0(10-15\text{ cm}).$$

Mean values, averaged over all sampling dates, were d_{50}(0–2 cm, 10–15 cm) = 571 μm $\pm$ 101 μm, d_{50}(2–10 cm) = 481 μm $\pm$ 83 μm, p_0(0–2 cm) = 0.374 $\pm$ 0.057, and p_0(2–15 cm) = 0.322 $\pm$ 0.020.

Bacteria and POC mineralisation

Bacterial cell numbers and depth distributions showed distinct seasonal changes (Figure 1). There was a subsurface maximum at 1.5–2.5 cm depth during summer (May, Jul, Sep) and at 3.0–4.5 cm depth during winter (Nov, Jan, Mar). Above this maximum, bacterial numbers steeply decreased towards the sediment surface (except for Nov 97), with minimum numbers attained at 0–2.5 cm depth. The gradient between this minimum and the subsurface maximum as well as the relative bandwidth, (max–min)/max, of cell numbers within a profile (Table 2) decreased in autumn and winter (Sep 97–Mar 98) and increased in spring and summer (Mar 98–Jul 98).

With an estimated mean cell diameter of 1 μm and a cellular organic carbon concentration of $1.1 \cdot 10^{-13}$ g μm^{-3} (Ritzrau & Graf 1992; Harvey et

Table 3. Particulate organic carbon (POC). Maximum content in the fine fraction, total amount in the upper 5 cm, and carbon mineralisation rates calculated from depth profiles of dissolved inorganic carbon (DIC). POC contents, DIC concentrations and computations were as per Rusch et al. (2000); also see explanations in the text. Significant correlations: $^{*}\alpha < 5\%$, $^{**}\alpha < 1\%$

	Maximum POC content % dwt.	Inventory (0–5 cm) g m^{-2}	Mineralisation rate mg C m^{-2} d^{-1}		
			B	C	D
Jul 97	4.90	31.7	201	519	
Sep 97	3.56	15.1	256	365	311
Nov 97	2.96	13.1	141		204
Jan 98	2.63	4.05	217	101	20
Mar 98	3.64	6.14	265	244	42
May 98	3.61	26.9	565	418	190
Jul 98	1.77	35.9	579	550	464
correlation to inventory	n.s.	**	*		

al. 1995), bacterial POC amounted to 3–22 μg (cm^3 sediment)$^{-1}$. By comparison, total sedimentary POC ranged between 32 and 2030 μg cm^{-3}, and median values of bacterial contribution to the sedimentary carbon pool ranged between 2.2% in July and 8.6% in January. In spite of this relatively small share, bacteria and POC appeared related to each other in various aspects. Throughout the year, the depth of maximum bacterial cell numbers was located between 1 cm above and 2 cm below the depth of fine particles richest in POC (Figure 1). Maximum bacterial numbers (Table 2) and maximum POC contents (Table 3) tended to be coupled, however not correlated. The same holds for the inventories (0–5 cm depth) of bacteria and POC.

The seasonal variation of carbon mineralisation rates (Table 3) appeared parallel to that of maximum bacterial cell numbers and numbers in 1–2 cm depth and 0–5 cm depth (Figure 2). However, the correlation between rates and these bacterial numbers was statistically not significant (Sachs 1997).

Figure 3 illustrates that organic-rich fine particles and optimum conditions for sedimentary bacteria were found in steadily deeper layers during autumn and winter and gradually closer to the sediment surface in the following spring and summer. Throughout the year, both maxima were located in the zone influenced by advective exchange across the water-sediment interface. The zone of DIC accumulation due to intense mineralisation narrowed in autumn and winter and expanded during spring and summer. From Nov 97 until Mar 98 it did not cover the depth of maximum bacterial cell numbers.

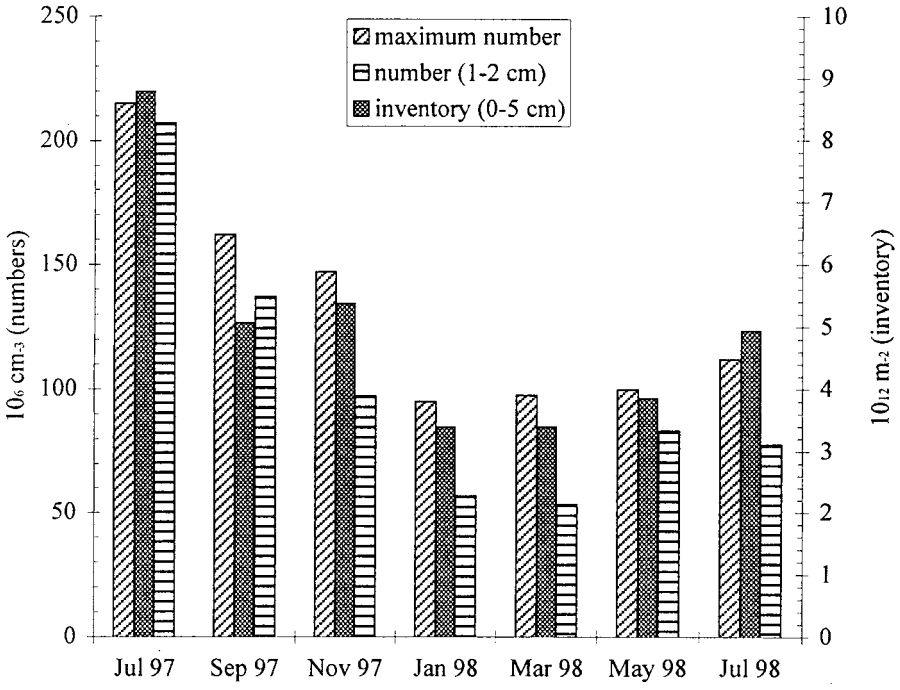

Figure 2. Seasonality of sedimentary bacteria: maximum numbers, inventory (0–5 cm), and numbers in the most active zone (1–2 cm depth).

Carbohydrates

The portion of sea water soluble and EDTA soluble carbohydrates was 0.92% ± 0.84% (n = 120) and 5.86% ± 4.01% (n = 120) of total carbohydrates, respectively. We observed no seasonal trend or characteristic depth profile in these data.

Total carbohydrate concentrations (Figure 4) varied only slightly with depth in winter (Jan 98, Mar 98), whereas the summer profiles (Jul 97, Sep 97, May 98, Jul 98) showed elevated concentrations in the uppermost 2–5 cm. Below 5 cm depth, only minor downcore or temporal changes occurred, and the mean concentration amounted to (1589 ± 830) μg cm^{-3} (n = 63). Carbohydrates in the upper 5 cm exceeding this background concentration were integrated for each sampling date (March: mean of 6 data sets). The resulting areal inventories (in g m^{-2}) steadily decreased from 130.7 in Jul 97 to 80.9 in Sep 97 and 66.2 in Jan 98, attained the minimum of –6.7 in Mar 98 and afterwards gradually increased to 18.0 in May 98 and 31.4 in Jul 98.

Carbohydrate inventories were not significantly correlated to either sediment permeabilities (Table 1) or the corresponding inventories of POC, PN

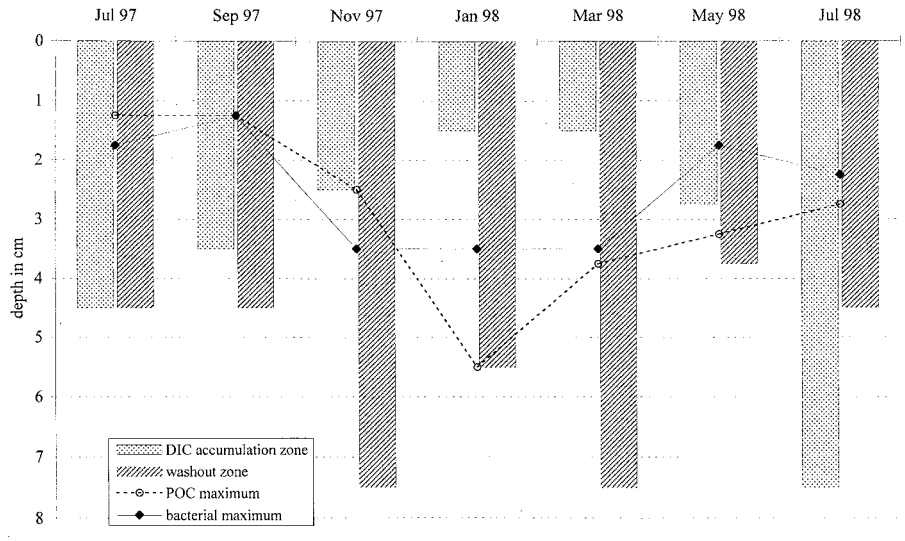

Figure 3. Horizons related to POC degradation. Hatched bars: depth interval from which fine-grained material was partially removed by hydrodynamic processes, with maximum concentrations of fine particles defining the lower end of this "washout" zone (Rusch et al. 2000). Stippled bars: zone of intense carbon mineralisation, defined as the depth interval of a local, cap-shaped DIC surplus superimposed on the basically linear depth profile. DIC was considered to accumulate during and near slack tide, whereas particle washout was rather associated with stronger ebb and flood currents in the tidal cycle. Circles: depth of maximum POC content of the fine fraction. Diamonds: depth of maximum bacterial cell numbers.

or Chl (data from Rusch et al. 2000). In several cores, however, total carbohydrate concentrations were significantly correlated to the concentrations of POC, Chl or bacteria (Table 4).

The difference between carbohydrate organic carbon (chOC) and POC(fine) can be used as a measure of the minimum amount of carbohydrates associated with the coarse fraction, if chOC – POC(fine) > 0. In our profiles, this difference was positive throughout the top 10 cm (except for 4 data points in May 98), revealing that there was more carbohydrate C_{org} in the coarse fraction than non-carbohydrate C_{org} in the fine fraction. With increasing sediment depth, chOC – POC(fine) tended to decrease. That means, adsorption of carbohydrates to the sand grains was less in deeper strata compared to above, or carbohydrate occurrence was selectively restricted to near-surface sediment, or both.

Diatoms

In our samples, most benthic diatoms were naviculoid. Planktonic diatoms were mainly centric, except for rod-shaped *Rhizosolenia* spec. and the

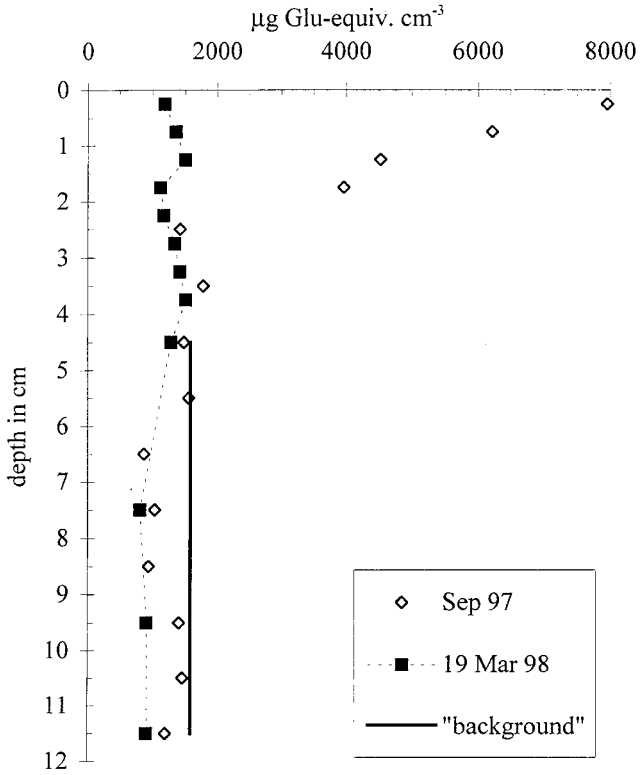

Figure 4. Depth profiles of total carbohydrate (given as glucose equivalent) concentrations. Diamonds: Sep 97 representing the summer situation; squares: 19 Mar 98 representing the winter situation; bold line: mean background concentration below 5 cm depth. The complete data set of all profiles is available from the authors.

almost brick-shaped, occasionally chain-forming *Brockmanniella brockmannii* (Hasle et al. 1983). The size class 15–20 μm was dominated by *B. brockmannii*, whereas no prominence of a certain family was observed in any other size class.

To improve the comparability of algal cell depth distributions, we present our data in terms of "relative particle numbers", i.e. diatom numbers in a certain depth interval divided by the total number of diatoms found in the core. Depth profiles could be classified into 3 major types, and a representative of each is shown in Figure 5. The dominant one was an exponential or linear decrease of relative particle numbers with depth (Figure 5a), a more or less even depth distribution of frustules (Figure 5b) occurred several times, and some profiles exhibited a subsurface maximum (Figure 5c). There was no general difference between the depth distributions of planktonic and

Table 4. Significant correlations between the concentrations of carbohydrates, POC, chlorophyll and bacteria

	POC	Chl	bacteria
Carbohydrates	Jul 97 (∗)	Jul 97 (∗∗)	Jul 97 (∗∗∗)
		Sep 97 (∗∗∗)	
		15 Mar 98 (∗)	
	Jul 98 (∗)	Jul 98 (∗∗)	Jul 98 (∗)
Chl	Jul 97 (∗)		
	Jul 98 (∗)		
Bacteria	Jul 97 (∗∗)	Jul 97 (∗∗∗)	
		15 Mar 98 (∗)	

$^{*}\alpha < 5\%$, $^{**}\alpha < 1\%$, $^{***}\alpha < 0.1\%$.

benthic diatoms ($\alpha < 10\%$, Wilcoxon matched pairs signed rank test, Sachs 1997), nor did depth distributions depend on cell size (Kruskal/Wallis test). However, a significant difference between the sampling dates was detected in the depth distributions of benthic ($\alpha < 1\%$) and planktonic ($\alpha < 0.1\%$) diatoms (Kruskal/Wallis test). In Jul 97, Nov 97, Jan 98 and 15 Mar 98, profiles were predominantly of the type shown in Figure 5a. Approximately even depth distributions (Figure 5b) were observed in Sep 97, 19 Mar 98 and 23 Mar 98, whereas a subsurface maximum (Figure 5c) occurred on 27 Mar 98 as well as in most profiles of May 98 and Jul 98.

The biovolume of benthic and planktonic diatoms was calculated from the numbers in each size class, approaching cell shapes in pervalvar view as rectangular (*B. brockmannii*), circular (other planktonic forms) or elliptic (benthic forms). The height of the frustule was estimated a quarter of its length. Diatom biovolumes were significantly correlated to POC concentrations in Sep 97 ($\alpha < 0.1\%$) and Jan 98 ($\alpha < 5\%$) as well as to Chl concentrations and bacterial numbers in Sep 97 ($\alpha < 5\%$). The inventories (0–5 cm) of diatom biovolume and carbohydrates were significantly ($\alpha < 5\%$) correlated with exception of Jan 98 and Mar 98. In each size class following the computation approaches given by Smayda (1978), diatom POC amounted to 10–170 μg (cm^3 sediment)$^{-1}$. Accordingly diatoms constituted 8–18%, in Mar 98 even 28%, of total sedimentary POC.

Photosynthetic pigments

Bacteriochlorophyll. HPLC analysis of our samples was unable to detect any BChl. Due to relatively small total bacterial numbers compared to a relatively

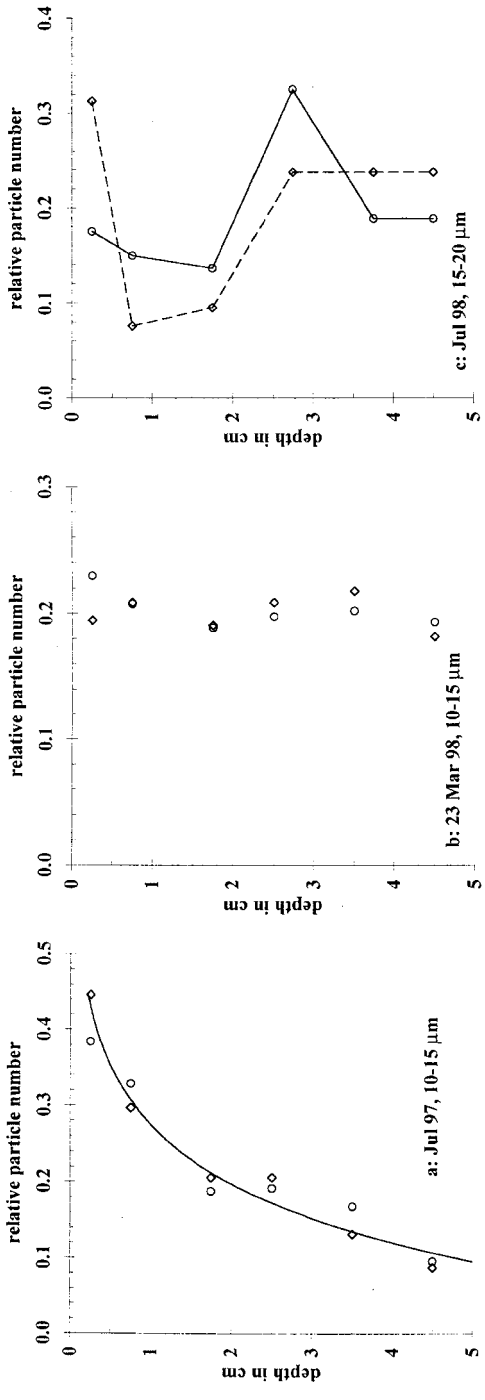

Figure 5. Depth profiles of relative particle numbers. Circles: planktonic diatoms, diamonds: benthic diatoms. a: exponential decrease, represented by Jul 97, 10–15 μm. b: even depth distribution, represented by 23 Mar 98, 10–15 μm. c: subsurface maximum, represented by Jul 98, 15–20 μm. The complete data set of all profiles is available from the authors.

high detection limit, no conclusion on the presence or absence of phototrophic microbes could be drawn.

Carotenoids. Detectable amounts of carotenoids were found in the samples of Jul 97, Sep 97 and Nov 97. They consisted of 40–100% fucoxanthin, 0–30% YA, 0–20% YC, and 0–20% others. Canthaxanthin, lutein and peridinin were below the detection limit. The share of hydrophobic carotenoids with long retention times tended to increase with sediment depth.

Chloropigments. Concentrations determined by fluorometry (Rusch et al. 2000) and by HPLC were significantly ($\alpha < 0.1\%$) correlated, with the slope of the regression line near unity.

For the following, the chloropigments were grouped into 3 sets. The hydrophobic set comprises chlorophyll and its early degradation products, pheophytin and XF (probably pheophorbide). XA and XB constitute the hydrophilic set, and the intermediate set consists of XC – XE. Figure 6 shows depth profiles of chloropigments based on fluorometric measurements, supplemented by HPLC data on the pigment composition. The portion of hydrophobic chloropigments, indicating barely degraded material, tended to decrease from the surface downwards. Especially high proportions in the uppermost layers and in the seston were observed in Jul 97, Sep 97, Mar 98 and Jul 98 (Figure 6) concurrent with phytoplankton blooms of *Phaeocystis globosa*, *Chaetoceros* spec., *Brockmanniella brockmannii* / *Skeletonema costatum* and *Phaeocystis globosa*, respectively. The chloropigments in the sediment surface layer were relatively rich in hydrophobic compounds in Jan 98, when *B.brockmannii* prevailed in the phytoplankton, however not forming a pronounced bloom. By contrast, suspended and sedimentary fine particles were dominated by intermediate and hydrophilic chloropigments in Nov 97 and May 98, indicating advanced degradation of phytodetritus.

Correlations. Except for the carotenoid YA, none of the pigment or pigment group concentrations were significantly ($\alpha < 5\%$) correlated to the diatom biovolume. Carbohydrate concentrations were significantly correlated to the hydrophilic ($\alpha < 5\%$) and the hydrophobic ($\alpha < 0.1\%$) chloropigments, but not to the intermediate ones. There was a highly significant ($\alpha < 0.1\%$) correlation between POC concentrations and each of the chloropigment sets.

Discussion

Besides catalysing a wide range of biogeochemical reactions, bacteria are part of the sedimentary POM pool and food web. Moreover, microbial exopoly-

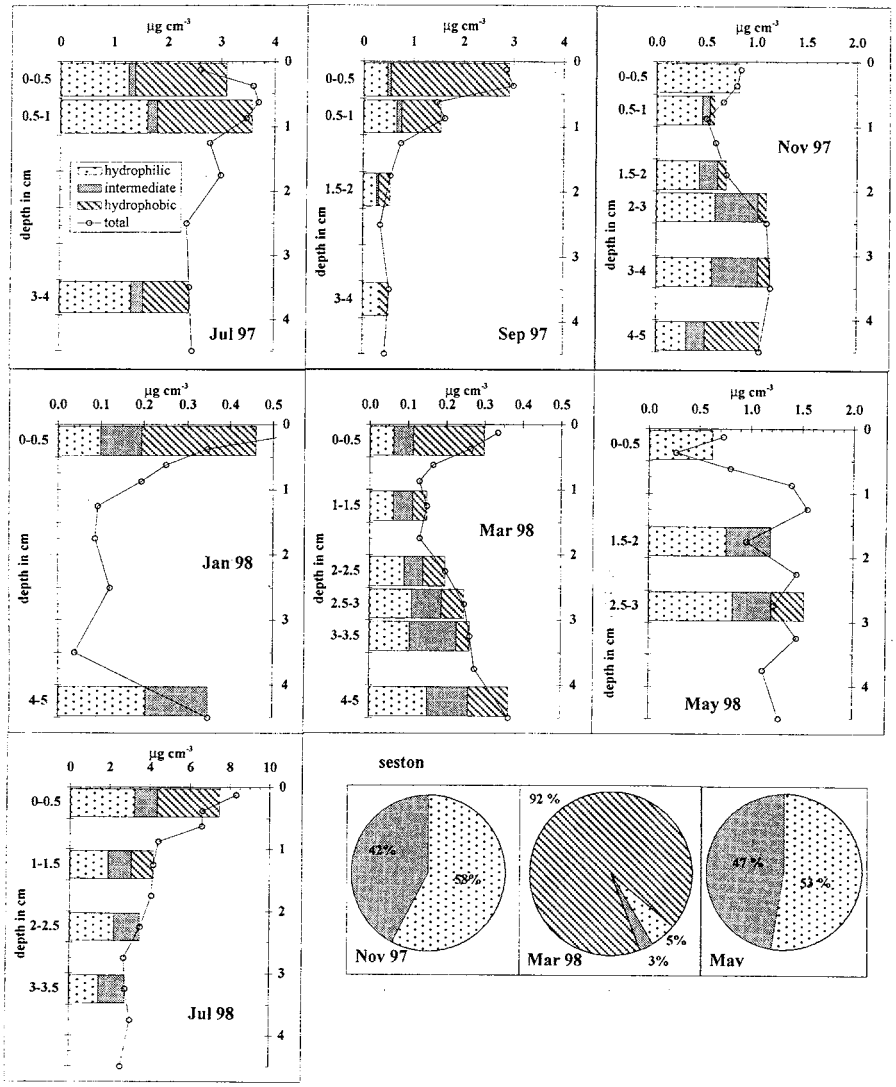

Figure 6. Depth profiles of chloropigment concentrations. Circles: total, hatched: hydrophobic, dark grey: intermediate, stippled: hydrophilic. Lower right panel: chloropigment composition of suspended particulate material in Nov 97, Mar 98 and May 98.

mers can alter the cohesivity of sediments (Grant & Gust 1987; Dade et al. 1990) and the adsorption of DOM and cells to the matrix (Decho & Lopez 1993). Both affect advective fluxes that depend on sediment permeability as well as on size and mobility of the transported particles, e.g. bacterial cells. In intertidal areas, the pronounced influences of seasons and water move-

ments add to the interactions between sedimentary bacteria and their dynamic environment.

Microbial particles subject to hydrodynamic forces

Unlike most depth distributions of bacteria reported in literature, with maximum cell numbers at the sediment surface (e.g. Sahm et al. 1999; Sievert et al. 1999), our profiles exhibited a subsurface maximum below a minimum (Figure 1). This characteristic feature was also found in the depth profiles of the fine fraction ($< 70\ \mu$m) and can be attributed to deep-reaching washout and subsequent particle trapping in the surface layer. Maximum bacterial numbers were observed 2–4 cm closer to the sediment-water interface than maximum concentrations of fine particulates (Figure 3), indicating somewhat lower susceptibility to hydrodynamic forces. Free-living single cells are most easily moved through the pore space and across the sediment surface. Bacteria attached to particles, however, benefit nutritionally over free-living forms by close association with an organic substrate and by increased solute flux due to fluid turbulence around the host particle (Logan & Kirchman 1991). In our permeable sand, advective pore water flows could provide solutes and turbulence, and bacteria were present on organic-rich fine particles and in the more protected habitat of microtopographic structures on coarse sand grains. With part of the microbial population attached to the coarse fraction ($> 70\ \mu$m), the bulk hydrodynamic mobility of sedimentary bacteria could fall short of that of the fine fraction. So maximum numbers of bacteria accumulated in a zone, where the bulk of small particles could not resist being carried out of the sediment (Figure 3).

The microbial population of our sandflat was highly dynamic in space and time, as shown by steep gradients and broad ranges within the profiles (Table 2) and by marked seasonal variations in the maximum number, the number in the most active zone and the inventory (Figure 2). Gradients and bandwidths gradually decreased from autumn until late winter (Mar 98) and increased in spring and summer, as location and size of the maximum varied seasonally. Due to decreasing food supply from above and hydrodynamic washout reaching deeper into the sediment, maximum bacterial numbers were found deeper in winter than in summer (Figure 3), thus making the gradient shallower. Lower maximum cell numbers (Table 2) added to this decrease of the gradient and furthermore narrowed the bandwidth. Conversely, in summer calmer hydrodynamic conditions, abundant food supply and higher maximum bacterial numbers increased both bandwidths and gradients. Apart from selection by interstitial water flows and availability of organic-rich particles acting on microbial life in a given sediment depth, bacteria may

also actively respond to seasonally changing conditions by moving towards an optimum depth.

Microbial organic matter

Strong correlations between bacteria and organic-rich fine particles may arise when microbial cells themselves are a major part of the sedimentary POC. This was not the case in our sandflat, with bacteria contributing less than 9% to the POC pool. Nor were POC compounds likely to be products of microbial primary production. Due to the HPLC detection limit and relatively small overall numbers of bacteria, our analyses failed to give clear evidence of the presence or absence of phototrophic bacteria. As the microbial contribution to photosynthetic pigments was undetectable, the microbial contribution to primary production was probably insignificant, too. Hence the main ecological role of our sandflat bacteria in organic matter turnover was degradation.

Microbial decomposition of organic matter

Although the standing stock of bacteria made only a minor contribution to sedimentary POC, cell numbers and POC were interlaced. Maxima adjoined each other (Figure 3) and seasonally developed in parallel, with bacteria lagging slightly (Tables 2 and 3) due to the dependence of heterotrophic microbial communities on organic matter supply. The coherence between bacteria and fine particles richest in POC may also imply that the major part of the microbes in our sandy sediment were attached to the interstitial fine fraction rather than to the organic-poor matrix. On the other hand, a bacterial population largely attached to sand grains, as suggested by their hydrodynamic mobility, profits from pore water DOC and prospers where organic-rich material is abundant, without neccessarily direct contact to the fine-grained POM. Optimum growth conditions could also contribute to make up for hydrodynamic losses and may serve as an additional explanation for the maintenance of high bacterial numbers within the reach of advective flushing (Figure 3).

Carbon turnover rates generally decreased from Jul 97 until Jan 98 and afterwards increased again, corresponding to the seasonal changes of the POC inventory (Table 3). The significant correlation between the potential of mineralisation and the actual rates emphasises tight coupling and effective use of the available POC. As both POC concentrations and temperatures were lower in winter, less bacteria could make their living (Figure 2) and mineralisation weakened (Table 3) compared to summer. The number of DAPI-stained cells, irrespective of their being dead or alive, decreased less

than carbon turnover rates, indicating that the surviving winter population consisted either of relatively many cells in reduced metabolic activity or of few cells in a fully active stage, probably something in between. The depths of highest numbers of bacteria and organic-richest fine particles increased towards the cold season and decreased in the following spring and summer (Figure 3). Optimum living conditions, as determined by hydrodynamically induced mechanical stress and by POC penetration, amount and quality, were found in deeper sediment layers throughout winter and closer to the surface in summer. The seasonality of organic matter degradation was revealed not only in rates (Table 3), but also in the depth range of intense DIC production (Figure 3). Remarkably, this DIC accumulation zone did not cover the depth of maximum cell numbers from Nov 97 till Mar 98, thus affirming the hypothesis of microbial dormancy in winter. Organic matter mineralisation was assessed by means of DIC depth profiles, and the approaches to calculate DIC production rates as well as the results on an annual basis are discussed elsewhere (Rusch et al. 2000). In the following we focus on the seasonality of mineralisation rates (Table 3) and the DIC accumulation zone (Figure 3). Carbon mineralisation rates in our coarse, organic-poor sand ranged between 20 and 579 mg C m^{-2} d^{-1}, whereas rates in a similar North Sea sediment were 60–192 mg C m^{-2} d^{-1} (Upton et al. 1993). We attribute these lower rates to measurements by core incubations that exclude advective oxidant supply and may, therefore, underestimate mineralisation rates in permeable sediments. Rates measured in fine sandy sediments of the North Sea and the Baltic Sea that were an order of magnitude richer in organic carbon than ours, ranged between 4 and 555 mg C m^{-2} d^{-1}, depending on season and location (Canfield et al. 1993; Upton et al. 1993; Kristensen & Hansen 1995; Osinga et al. 1996; Boon & Duineveld 1998; Boon et al. 1998). In these finer-grained sediments, permeability may have limited advective interfacial flows that both remove reduced metabolites and supply oxidants. By contrast, coarser sands like ours facilitated more intense and deeper-reaching exchange across the water-sediment interface, thereby enhancing turnover (Forster et al. 1996; Reimers et al. 1996; Huettel et al. 1998). The relatively low organic carbon contents of non-accumulating permeable sediments are therefore considered also a consequence of rapid mineralisation.

Diatoms as sedimentary organic matter

In marine ecosystems diatoms act as primary producers, but they may also live heterotrophically for several days (Harvey et al. 1995; Nelson et al. 1999), and they can constitute a major part of the POM in the water column and the sediment. Total POC concentrations in our sandflat ranged between 32 and 2030 μg cm^{-3}, with bacteria contributing up to 22 μg cm^{-3} and

diatoms up to 170 μg cm^{-3}. Thus, diatom carbon was not negligible, though the main part of sedimentary POC was detritus or adsorbed extracellular substances, both possibly derived from diatoms.

The depth distribution of diatom frustules did not significantly differ between planktonic and benthic forms, suggesting similar mobility on the scale of our depth resolution. In sandy sediments moderately exposed to waves and currents, attached benthic diatoms generally dominate over motile ones (Asmus & Bauerfeind 1994). On the other hand, sandflat diatoms can actively move vertically with an amplitude of several cm, controlled by wave energy, light and chemical gradients (Kingston 1999). We detected no significant difference between the depth distributions of differently sized diatoms, as given the studied size range of diatoms, the spatial resolution of the depth profiles was insufficient.

Depth distributions depended on the sampling date, forming 3 profile types (Figure 5). Relative particle numbers decreasing exponentially with depth were observed, when supply from above exceeded degradation, either due to diatom blooms (Jul 97, *Rhizosolenia imbricata*) or because of low temperatures slowing down degradation (Jan 98, 15 Mar 98). When supply and removal were balanced, profiles were vertical. The 1998 diatom spring bloom was followed by a summer poor in diatom phytoplankton and favouring decomposition and hydrodynamic removal, causing a subsurface maximum of relative particle numbers (Figure 5c). Phytoplankton blooms generally provide large numbers of monospecific, almost equally sized cells, and thus, *B. brockmannii* frustules from the 1997 and 1998 spring blooms dominated the 15–20 μm size class in our samples. The 1997 summer and autumn blooms, however, failed to become likewise evident, as they were far less pronounced and apparently insufficient to prevail among the older frustules accumulated in the sediment.

Shortly after a diatom bloom in Sep 97, diatom biovolumes were significantly correlated to POC and Chl concentrations, supporting that diatoms were a major source of sedimentary organic carbon. During the rest of the year this relation was less prominent, as different degrees of hydrodynamic mobility and biogeochemical lability of diatoms, organic carbon and Chl interfered. The significant correlation between diatom and carbohydrate inventories emphasises diatoms as the main provenance of intra- and extracellular carbohydrates.

Sedimentary organic matter

Phytopigments are widely used as biomarkers to trace transport or degradation pathways of algal material or to reveal the origin of phytodetritus, the major food source of heterotrophic microbenthos. In this study, chloropig-

ment concentrations served as a measure of the amounts of relatively fresh algal material; chloropigment composition was used to assess its state of degradation, carotenoid composition revealed the contribution of certain algal classes, and bacteriochlorophyll was used to estimate the number of phototrophic bacteria. Generally canthaxanthin serves as a biomarker for cyanobacteria, peridinin for Dinophyceae, and lutein for Rhodophyceae and Chlorophyceae (Goodwin 1980; Bianchi et al. 1988; Rowan 1989; Abele-Oeschger 1991; Steenbergen et al. 1994). As none of these carotenoids was detected, we conclude that cyanobacteria, dinoflagellates and macroalgae constituted a negligible part of the phytodetritus and phytobenthos in our sandflat. Fucoxanthin or close derivatives are the major carotenoid of Bacillariophyceae, Haptophyceae and Phaeophyceae (Goodwin 1980; Rowan 1989; Abele-Oeschger 1991). They were prevalent in our samples, corresponding to the dominance of diatoms in Königshafen phytoplankton and phytobenthos at sandy sites (Asmus & Bauerfeind 1994) or to detrital *Fucus* spec. growing in other parts of the bay (Schories et al. 1997). The apparent absence of carotenoids in the second summer of our study may be explained by a combination of low algal cell numbers (see above) with the relatively high detection limit.

Chloropigments, especially the most hydrophobic ones, proved to be good indicators of sedimentary organic matter, as they were significantly correlated to POC and carbohydrates. However, there was no correlation to the diatom biovolume, probably because the decomposition of frustules was much slower than that of pigments.

The set of hydrophobic chloropigments (chlorophyll, pheophytin, pheophorbide) was used as a marker for relatively fresh material. In most profiles, their contribution to total pigments tended to decrease downcore, but they were often present even at 4–5 cm depth (Figure 6). This deep penetration of fresh phytodetritus demonstrated the close link between the water column and at least the uppermost 5 cm of our permeable sediment. Likewise temporally, seston composition and phytoplankton blooms were closely related to the sedimentary chloropigment composition. Chlorophyll, albeit the most labile fraction of organic matter (Henrichs & Doyle 1986), was entered and transported through the upper sediment strata more quickly than it decomposed. This emphasises the efficiency of interfacial and subsurface particle transport by advection, considered a major mechanism in our sandflat, whereas bioturbation and ripple migration were less important (Rusch et al. 2000).

Several depth profiles of Chl concentration had subsurface maxima (Figure 6), that can be attributed to the same hydrodynamic processes that caused subsurface maxima in bacterial cell numbers (Figure 1) and the concentration of fine particulate material. Subsurface Chl maxima were occa-

sionally detected in the finer-grained sediments of Long Island Sound, USA (Sun et al. 1991; Sun et al. 1994), and at two North Sea sites exposed to near-bottom water currents of up to 0.25 m s^{-1} (Frisian Front) and up to 0.45 m s^{-1} (Broad Fourteens) over a fine sandy bottom and over medium coarse sand, respectively (Boon & Duineveld 1998). In Long Island Sound they were explained as a consequence of rates and mechanisms of decay varying with depth, seasonally changing input, and non-diffusive vertical transport by conveyor-belt feeders (Sun et al. 1991; Sun et al. 1994). Non-local mixing was considered a major cause at the North Sea locations, particularly at the Frisian Front station abundant in macrozoobenthos, and advective transport possibly enhanced interfacial particle fluxes at station Broad Fourteens (Boon & Duineveld 1998). We suggest that generally the deep penetration of fine-grained POM is advectively enhanced in permeable sandy shelf sediments subject to moderate near-bottom currents. Furthermore, resuspension and depth-dependent decomposition, both enhanced advectively as well, may partially remove near-surface POM and thereby cause a subsurface maximum.

Carbohydrates produced and consumed by bacteria

Besides intracellular storage polysaccharides, copious amounts of exopolymeric substances (EPS) are produced by aquatic micro-organisms, benthic diatoms, benthic fauna and colony-forming planktonic algae. Capsule EPS high in glycoproteins are primarily produced during the log phase of growth, whereas mucus EPS are largely polysaccharide and mainly secreted in the stationary phase or during nutrient limitation (Decho & Lopez 1993). Their various ecological functions include cell attachment, locomotion, protection from desiccation or digestion, and sorption of solutes and colloidal compounds (Decho & Lopez 1993; Underwood et al. 1995; Smith & Underwood 1998).

Former studies of sedimentary polysaccharides, mainly dealing with microbial or diatom mats, have focused on the uppermost centimetre. We show profiles of carbohydrates in a sandy marine sediment down to 12 cm depth (Figure 4).

The sea water soluble fraction, containing diatom motility polysaccharides (Underwood et al. 1995), comprised only 1% of the carbohydrates in our Sylt sediment. This labile DOC may have been degraded rapidly in the sediment and might be removed by pore water flows, as the study site was submerged until sampling. The EDTA extractable fraction, containing more tightly bound EPS, bacterial capsular EPS and some intracellular carbohydrates due to cell leakage (Underwood et al. 1995), amounted to 5.9% of the carbohydrates in our sandflat. Accordingly, the vast majority

of sedimentary polysaccharides was intracellular or very tightly bound to particles. With increasing proximity to the sediment surface, i.e. increasing hydrodynamic impact, carbohydrates tended to be increasingly adsorbed to the coarse sand grains and decreasingly to the fine fraction, that was more susceptible to resuspension and advective removal from the sediment.

In winter, total carbohydrate concentration profiles were almost vertical, whereas in summer, elevated concentrations were found in the uppermost 2–5 cm (Figure 4). The concentrations in winter or below 5 cm depth represented the refractory part, and planktonic and benthic primary production in summer added more easily degradable material to the upper 5 cm of the sediment. In summer 1998, there were less carbohydrates than in summer 1997, with a corresponding interannual difference in bacterial inventories (Figure 2). The second summer of our study was characterised by stronger winds, less sunshine and lower temperatures than the first one (Deutscher Wetterdienst 1998, unpubl. data), so polysaccharide production in the course of overflow metabolism (Staats 1999) was less pronounced. Throughout the year, significantly correlated concentrations were detected most often between carbohydrates and Chl (Table 4), indicating their similarly high lability. The concentrations of the more refractory bulk POC were correlated to the other OM indicators only in Jul 97 and Jul 98 (Table 4), when labile components dominated sedimentary POC.

Permeable sediments as microbial habitat

Maximum numbers of bacteria were found neither at the sediment surface nor associated with largest amounts of sedimentary POM, but with the organic-richest fine particles (Figure 3). Intense carbon turnover (Table 3) catalysed by the relatively small microbial population of an organic-poor sand was facilitated by the deep penetration of POM and oxidants into the sediment. In permeable, non-accumulating sands, solute and particle fluxes across the water-sediment interface are enhanced by advection, with sediment permeability among the main factors controlling transport rates and penetration depths (Forster et al. 1996; Huettel et al. 1996; Shum & Sundby 1996). Sediment permeabilities may be modified by exopolysaccharides, but in our sandflat, carbohydrate concentrations were relatively low and apparently insufficient to cause measurable changes in permeability, as evident in the lack of significant correlation. Although sediment permeability varied temporally, it appeared unrelated to the seasons. Throughout the year only minor changes occurred in the fine particle concentration below 5 cm depth, so seasonal changes in the grain size distribution of the top 5 cm had no clearly measurable effect on the permeability of a 15–20 cm long core. Most marine sediments are characterised by grain size and porosity, and there are several empirical

approaches to estimate permeability from granulometric data. We compared measured permeabilities to calculated ones (Table 1) and found no satisfactory conformity. Although both k_{KM} and k_H were significantly correlated to k with a slope near unity, there was a considerable offset, so that calculated values were about 4 times the measured ones. The Carman/Kozeny approach, applicable to almost spherical, well-sorted grains (Nield & Bejau 1992), yielded 5 times the measured permeabilities. Equations predicting aquifer permeabilities from grain size generally give poor estimates (Eggleston & Rojstaczer 1998), with errors often more than an order of magnitude (Shepherd 1989). Logarithmic scaling and interpolation to determine d_{10}, d_{50} and $\sigma(\phi)$ may have introduced a relative error of 0.1 each, and with an estimated relative error of 0.05 in the determination of p_0, these errors added up to 0.68, 0.45 and 0.20 for k_{KM}, k_{CK} and k_H, respectively. Moreover, the sediment cores had possibly been compacted by sampling, and some experimental error was added by the measuring system. But these errors still fail to explain all of the discrepancy. Therefor, we prefer to rely on direct measurements rather than on the estimation approaches.

Conclusions

Shallow water sediments like those in the sandflat we studied are often exposed to strong near-bottom water currents and are well-supplied with POM from the euphotic zone. Their high permeability facilitates deep-reaching advective transport of POM, oxidants, bacteria and degradation products into and out of the sediment.Sandy continental shelf sediments, thus, may play an important role in marine organic matter turnover in spite of their low organic content. In an intertidal sandflat previously characterised as strongly influenced by advective interfacial and subsurface flows, we have used phytopigments to show the close link between water column and the uppermost 5 cm of the sediment. The microbial population was highly dynamic spatially and temporally and rapidly mineralised organic matter, supplied by advectively enhanced interfacial fluxes of solutes and particles. The hydrodynamic influence was also revealed in the adsorption of carbohydrates to the coarse sand matrix, which increased towards the sediment surface. Together with earlier data from the same study (Rusch et al. 2000) and various significant correlations, our investigations have sketched a coherent picture of the circumstances, organisms, substances and processes involved in the ecologically significant biogeochemistry of sandy intertidal sediments.

Acknowledgements

We thank M. Alisch for her help during field work and the BAH Wadden Sea Station for providing lab space and detailed information on Königshafen. Deutscher Wetterdienst (DWD) kindly placed local weather data throughout the study period at our disposal. We acknowledge F. Garcia-Pichel and J. Zopfi for providing pigment standards and advice in HPLC analysis and appreciate valuable discussions with B. B. Jørgensen. Two anonymous reviewers helped to improve the manuscript. This study was supported by the Max Planck Society (MPG), and A. R. received a postgraduate scholarship from Deutsche Forschungsgemeinschaft (DFG).

References

Abele-Oeschger D (1991) Potential of some carotenoids in two recent sediments of Kiel Bight as biogenic indicators of phytodetritus. Mar. Ecol. Prog. Ser. 70: 83–92

Asmus RM & Bauerfeind E (1994) The microphytobenthos of Königshafen – spatial and seasonal distribution on a sandy tidal flat. Helgol. Meeresunters. 48: 257–276

Bianchi TS, Dawson R & Sawangwong P (1988) The effects of macrobenthic deposit-feeding on the degradation of chloropigments in sandy sediments. J Exp. Mar. Biol. Ecol. 122: 243–255

Boon AR & Duineveld GCA (1998) Chlorophyll a as a marker for bioturbation and carbon flux in southern and central North Sea sediments. Mar. Ecol. Prog. Ser. 162: 33–43

Boon AR, Duineveld GCA, Berghuis EM & van der Weele JA (1998) Relationships between benthic activity and the annual phytopigment cycle in near-bottom water and sediments in the Southern North Sea. Est. Coast. Shelf Sci. 46: 1–13

Canfield DE, Thamdrup B & Hansen JW (1993) The anaerobic degradation of organic matter in Danish coastal sediments: Iron reduction, manganese reduction, and sulfate reduction. Geochim. Cosmochim. Acta 57: 3867–3883

Dade WB, Davis JD, Nichols PD, Nowell ARM, Thistle D, Trexler MB & White DC (1990) Effects of bacterial exopolymer adhesion on the entrainment of sand. Geomicrobiol. Journal 8: 1–16

Darcy HPG (1856) Les Fontaines Publiques de la Ville de Dijon. Victor-Dalmont, Paris

Decho AW & Lopez GR (1993) Exopolymer microenvironments of microbial flora: Multiple and interactive effects on trophic relationships. Limnol. Oceanogr. 38: 1633–1645

Eggleston J & Rojstaczer S (1998) Inferring spatial correlation of hydraulic conductivity from sediment cores and outcrops. Geophys. Res. Letters 25: 2321–2324

Epstein SS & Rossel J (1995) Enumeration of sandy sediment bacteria: search for optimal protocol. Mar. Ecol. Prog. Ser. 117: 289–298

Flemming BW & Ziegler K (1995) High-resolution grain size distribution patterns and textural trends in the backbarrier environment of Spiekeroog Island (southern North Sea). Senckenbergiana maritima 26: 1–24

Forster S, Huettel M & Ziebis W (1996) Impact of boundary layer flow velocity on oxygen utilization in coastal sediments. Mar. Ecol. Prog. Ser. 143: 173–185

Gätje, C. & Reise, K. (1998) Ökosystem Wattenmeer: Austausch-, Transport- und Stoffumwandlungsprozesse. Springer, Berlin

Goodwin TW (1980) The Biochemistry of the Carotenoids. Chapman & Hall
Grant J & Gust G (1987) Prediction of coastal sediment stability from photopigment content of mats of purple sulphur bacteria. Nature 330: 244–246
Harvey HR, Tuttle JH & Bell JT (1995) Kinetics of phytoplankton decay during simulated sedimentation: Changes in biochemical composition and microbial activity under oxic and anoxic conditions. Geochim. Cosmochim. Acta 59: 3367–3377
Hasle GR, von Stosch HA & Syvertsen EE (1983) Cymatosiraceae, a new diatom family. Bacillaria 6: 9–156
Henrichs SM & Doyle AP (1986) Decomposition of ^{14}C-labelled organic substances in marine sediments. Limnol. Oceanogr. 31: 765–778
Hsü KJ (1989) Physical Principles of Sedimentology. Springer, Berlin
Huettel M & Gust G (1992) Impact of bioroughness on interfacial solute exchange in permeable sediments. Mar. Ecol. Prog. Ser. 89: 253–267
Huettel M, Ziebis W & Forster S (1996) Flow-induced uptake of particulate matter in permeable sediments. Limnol. Oceanogr. 41: 309–322
Huettel M, Ziebis W, Forster S & Luther III GW (1998) Advective transport affecting metal and nutrient distributions and interfacial fluxes in permeable sediments. Geochim. Cosmochim. Acta 62: 613–631
Karsten U & Garcia-Pichel F (1996) Carotenoids and mycosporine-like amino acid compounds in members of the genus *Microcoleus* (cyanobacteria): a chemosystematic study. Systematic and Applied Microbiology 19: 285–294
Kingston MB (1999) Wave effects on the vertical migration of two benthic microalgae: *Hantzschia virgata* var. *intermedia* and *Euglena proxima*. Estuaries 22: 81–91
Klute A & Dirksen C (1986) Hydraulic conductivity and diffusivity: laboratory methods. In: Klute A (Ed.) Methods of Soil Analysis – part 1 – Physical and Mineralogical Methods (pp 687–700). American Society of Agronomy
Kristensen E & Hansen K (1995) Decay of plant detritus in organic-poor marine sediment: production rates and stoichiometry of dissolved C and N compounds. J Mar. Res. 53: 675–702
Logan BE & Kirchman DL (1991) Uptake of dissolved organics by marine bacteria as a function of fluid motion. Mar. Biol. 111: 175–181
Nelson JR, Eckman JE, Robertson CY, Marinelli RL & Jahnke RA (1999) Benthic microalgal biomass and irradiance at the sea floor on the continental shelf of the South Atlantic Bight: Spatial and temporal variability and storm effects. Cont. Shelf Res. 19: 477–505
Nield DA & Bejau A (1992) Convection in Porous Media. Springer, Berlin
Osinga R, Kop AJ, Duineveld GCA, Prins RA & van Duyl FC (1996) Benthic mineralization rates at two locations in the southern North Sea. J Sea Res. 36: 181–191
Pankow H (1990) Ostsee-Algenflora. Gustav-Fischer-Verlag, Jena
Pilditch CA, Emerson CW & Grant J (1998) Effect of scallop shells and sediment grain size on phytoplankton flux to the bed. Cont. Shelf Res. 17: 1869–1885
Reimers CE, Glenn SM & Creed EL (1996) The dynamics of oxygen uptake by shelf sediments. EOS 76: OS202
Ritzrau W & Graf G (1992) Increase of microbial biomass in the benthic turbidity zone of Kiel Bight after resuspension by a storm event. Limnol. Oceanogr. 37: 1081–1086
Rowan KS (1989) Photosynthetic Pigments of Algae. Cambridge University Press, Cambridge
Rusch A, Huettel M & Forster S (2000) Particulate organic matter in permeable marine sands – dynamics in time and depth. Est. Coast. Shelf Sci. 51: 399–414
Sachs L (1997) Angewandte Statistik. Springer, Berlin

Sahm K, MacGregor BJ, Jørgensen BB & Stahl DA (1999) Sulphate reduction and vertical distribution of sulphate-reducing bacteria quantified by rRNA slot-blot hybridization in a coastal marine sediment. Env. Microbiol. 1: 65–74

Schories D, Albrecht A & Lotze H (1997) Historical changes and inventory of macroalgae from Königshafen Bay in the northern Wadden Sea. Helgol. Meeresunters. 51: 321–341

Shepherd RG (1989) Correlations of permeability and grain size. Ground Water 27: 633–638

Shum KT & Sundby B (1996) Organic matter processing in continental shelf sediments – the subtidal pump revisited. Mar. Chem. 53: 81–87

Sievert SM, Brinkhoff T, Muyzer G, Ziebis W & Kuever J (1999) Spatial heterogeneity of bacterial populations along an environmental gradient at a shallow submarine hydrothermal vent near Milos Island (Greece). Appl. Env. Microbiol. 65: 3834–3842

Smayda TJ (1978) From phytoplankters to biomass. In: Sournia A (Ed.) Phytoplankton Manual (pp 273–279). UNESCO, Paris

Smith DJ & Underwood GJC (1998) Exopolymer production by intertidal epipelic diatoms. Limnol. Oceanogr. 43: 1578–1591

Staats N (1999) Exopolysaccharide production by marine benthic diatoms. Ph.D. thesis, University of Amsterdam

Steenbergen CLM, Korthals HJ & Dobrynin EG (1994) Algal and bacterial pigments in non-laminated lacustrine sediment: studies of their sedimentation, degradation and stratigraphy. FEMS Microbiol. Ecol. 13: 335–352

Sun M, Aller RC & Lee C (1991) Early diagenesis of chlorophyll-a in Long Island Sound sediments: A measure of carbon flux and particle reworking. J Mar. Res. 49: 379–401

Sun M, Aller RC & Lee C (1994) Spatial and temporal distributions of sedimentary chloropigments as indicators of benthic processes in Long Island Sound. J Mar. Res. 52: 149–176

Underwood GJC, Paterson DM & Parkes RJ (1995) The measurement of microbial carbohydrate exopolymers from intertidal sediments. Limnol. Oceanogr. 40: 1243–1253

Upton AC, Nedwell DB, Parkes RJ & Harvey SM (1993) Seasonal benthic microbial activity in the southern North Sea; oxygen uptake and sulphate reduction. Mar. Ecol. Prog. Ser. 101: 273–281

Yallop ML, de Winder B, Paterson DM & Stal LJ (1994) Comparative structure, primary production and biogenic stabilization of cohesive and non-cohesive marine sediments inhabited by microphytobenthos. Est. Coast. Shelf Sci. 39: 565–582

Ziebis W, Huettel M & Forster S (1996) Impact of biogenic sediment topography on oxygen fluxes in permeable sediments. Mar. Ecol. Prog. Ser. 140: 227–237